ARTICLE

Self-assembly of Binary Particles with Electrostatic and van der Waals Interactions

Yan Li[a], Hua-ping Li[b], Xue-hao He[a]*

a. Department of Chemistry, School of Science, Tianjin University, and Collaborative Innovation Center of Chemical Science and Engineering, Tianjin 300072, China
b. Department of Polymer Science and Engineering, School of Chemical Engineering and Technology, Tianjin University, Tianjin 300072, China

(Dated: Received on April 3, 2014; Accepted on July 2, 2014)

Nanoparticles with competitive interactions in solution can aggregate into complex structures. In this work, the synergistic self-assembles of binary particles with electrostatic and van der Waals interactions are studied with the particle Langevin dynamics simulation using a simple coarse-grained particle model. Various aggregations such as spherical, stacking-disk and tube structures are observed by varying the particles size and the interaction strength. The aggregation structures are explained with the packing theories of amphiphilic molecules in solution and dibolck copolymers in bulk. When the opposite ions are introduced into solution, the distribution of structures in the phase diagram appears an obvious offset. The simulation result is helpful to deeply understand the formation mechanism of complex nanostructures of multicomponent particles in solution.

Key words: Repulsive interaction, Self-assembly, Binary particles, Particle dynamics, Phase diagrams

I. INTRODUCTION

Nanostructures formed through the self-assembly of particles have attracted much attention and have wide applications such as the identification of molecules, the data storage, the recovery of catalysts, electrochemical biosensors, electronic and optoelectronic devices [1−8]. The novel and hierarchy structures bring extraordinary properties in physics and chemistry. Instead of using single component particles, nanostructures from multicomponent particles can integrate the properties of each component and show synergistic characters far beyond those of their individual section [9−12]. Using the diverse fabrication methodologies (*e.g.*, wet-chemical techniques, the template-directed method and applications of external driving fields), various ordered structures, including nanorods [10, 13−15], nanowires [16, 17], nanospheres [18−27], nanotubes [28, 29], nanocrystals [30], and hierarchic structures [31] from particle self-assembly have been fabricated. Prominent physical and chemical properties such as extraordinary semiconducting characters [14, 19], particular optical effects [28−30], and strong catalysis activities [13, 18, 27] can be achieved. Compared with the top-down fabrication technology, the self-assembly (bottom-up) method has prominent advantages in manufacturing advanced materials with ordered structures. How to synergistically tune the self-assembly structure of particles has been one of the most important tasks in the field of nanotechnology.

Past experiments have demonstrated that the particles self-assembly under hybrid interactions can create rich aggregation structures [32−37]. When the charged particles are introduced, the hierarchy structures are widely discovered. Compared with the common van der Waals attraction which only leads to indiscriminate "sticking" interaction, the electrostatic interactions richen the competition interaction between particles [38]. It is shown that the formation of complex structures sensitively depends on the particle size, concentration and interaction strength [39−54]. It is still difficult to fully explain and predict the nanostructures formation in multicomponent systems using currently experimental and theoretical methods [55, 56] while past researches only explored the influence of partial factors on the self-assembly [39, 40, 44, 45, 52]. Compared with experimental methods, the molecular simulation can achieve detail information on molecular scales in the aggregation process or chemical reactions [57, 58]. The systematical simulation study on the effects of electrostatic and van der Waals interactions together with the particles size is rare [34].

The binary particles system as the simplest multicomponent system has the fundamental importance in understanding the nanostructure formation of multicomponent particles. How the van der Waals attraction

*Author to whom correspondence should be addressed. E-mail: xhhe@tju.edu.cn, Tel./FAX: +86-22-27404303

and the electrostatic repulsion between different type particles affect the formation of the self-assembly structure in a binary particles system is an interesting question. In this work, the particle Langevin dynamics (LD) simulation with a general coarse-grained particle model is implemented to explore the formation of complex nanostructures in the system with binary particles (A and B types of particles). Different from the past simulation researches [34, 45, 59], the synergistic self-assembly of binary particles with repulsive electrostatic and attractive van der Waals interactions is explored. In present system, A particles have the common van der Waals interaction and B particles are charged as ions or charged particles. Two cases for B particles with the same charges or opposite charges are considered. A strong cross-interaction between A and B particles is employed to reflect the synergistic effect between binary components. The annealing method is applied in the simulation to achieve the equilibrium structures. The phase diagrams depending on the particle sizes are finally achieved. Inspired by the packing theory of amphiphilic molecules or diblock copolymers in solution or bulk systems, we explain the self-assembly structures in a similar way. Our simulation results are valuable to deeply understand the formation of complex nanostructures and to effectively predict the synergistic self-assembly for multicomponent particles systems with strong cross-interactions.

II. SIMULATION

The particle LD with the implicit solvent is used to effectively simulate the aggregation process of binary particles in solution. The system contains two kinds of particles (type A and B). The van der Waals attraction interaction (using the Lennard-Jones type potential) exists between A particles or A and B particles. Meanwhile, B particles are charged to introduce the electrostatic force. Two cases are considered: (i) all B particles have the same negative charges, *i.e.*, only repulsive interaction exists between B particles; (ii) B particles are divided into two classes which have the opposite charges (the system is electrically neutral). In the second case, the weak van der Waals interaction between B particles is added to avoid the attraction singularity.

The van der Waals interaction $U_{\rm LJ}(r_{ij})$ in this work has the form:

$$U_{\rm LJ}(r_{ij})=\begin{cases} V(r_{ij}), & r_{ij}<r_1 \\ V(r_{ij})+S(r_{ij}), & r_1\le r_{ij}\le r_{\rm c} \\ 0, & r_{ij}>r_{\rm c} \end{cases} \quad (1)$$

$$V(r_{ij})=4\varepsilon_{ij}\left[\left(\frac{\sigma_{ij}}{r_{ij}}\right)^{12}-\left(\frac{\sigma_{ij}}{r_{ij}}\right)^{6}\right] \quad (2)$$

$$S(r_{ij})=\int_{r_1}^{r_{\rm c}} F_S(x){\rm d}x \quad (3)$$

$$F_S(r_{ij})=k_1(r_{ij}-r_1)^2+k_2(r_{ij}-r_1)^3 \quad (4)$$

where r_1=4.2 nm, $r_{\rm c}$=4.3 nm, $V(r_{ij})$ is the pure Lennard-Jones potential, ε_{ij} is the interaction intensity of the Lennard-Jones potential for particles, σ_{ij} is the diameter of particles, r_{ij} is the distance between the centers of two particles, $S(r_{ij})$ and $F_S(r_{ij})$ are the shifted potential and shifted force, respectively. $r_{\rm c}$ is the cut-off value for van der Waals interactions of two particles. To ensure the shift function smoothly at the boundaries, the boundary conditions are imposed: $S'(r_1)$=0, $S''(r_1)$=0, $S'(r_{\rm c})$=$-V'(r_{\rm c})$, $S''(r_{\rm c})$=$-V''(r_{\rm c})$. The parameters k_1 and k_2 can be calculated from the boundary conditions. The electrostatic interaction $U_{\rm crf}(r_{ij})$ has the form:

$$U_{\rm crf}(r_{ij})=\begin{cases} f\dfrac{q_iq_j}{\varepsilon_{\rm r}}\left(\dfrac{1}{r_{ij}}-\dfrac{1}{r_{\rm crf}}\right), & r_{ij}\le r_{\rm crf} \\ 0, & r_{ij}>r_{\rm crf} \end{cases} \quad (5)$$

which is shifted to zero at $r_{\rm crf}$=4.45 nm. Here, f is the electric conversion factor and f=$1/(4\pi\varepsilon_0)$= 138.94 (kJ nm)/(mol e^2), ε_0 is the vacuum dielectric constant, $\varepsilon_{\rm r}$ is the relative dielectric constant, $\varepsilon_{\rm r}$=78, and q is the charge of one particle.

In this work, $\sigma_{\rm AA}$ and $\sigma_{\rm AB}$ were varied from 0.1 nm to 2 nm to simulate the self-assembly of low scale nanoparticles in a mesoscopic solution system. $\varepsilon_{\rm AA}$=4 kJ/mol, $\varepsilon_{\rm AB}$=10 kJ/mol were selected. The aggregation of particles would not occur if the attraction strength was too weak and the computation would not be stable if a strong attraction was used. The charges of B particles are set as $q_{\rm B}$=$-$0.6e in the case of same charges and $q_{\rm B}$=$\pm$0.6e in the case of opposite charges. For B particles with opposite charges, the weak van der Waals interaction with $\sigma_{\rm BB}$=0.1 nm, $\varepsilon_{\rm BB}$=0.1 kJ/mol was used. However, there was not van der Waals interaction between the same charged B particles.

The particle Langevin dynamics simulation was implemented with Gromacs 4.5 (the integrator of stochastic dynamics is chosen) [60]. At the beginning of the simulation, 400 A particles and 5800 B particles were distributed randomly in a box of size 27 nm×27 nm× 27 nm (the concentrations of A and B particles were 0.03 and 0.49 mol/L, respectively). The annealing method from a high temperature (corresponding to a dispersed state) to the room temperature (300 K) was used to achieve the equilibrium structures. The temperature coupling time constant τ_t of 0.1 ps and the time step Δt of 0.01 ps were used. The simulation time was up to 5 μs. The aggregation structures were shown with the visual molecular dynamics (VMD) package.

III. RESULTS AND DISCUSSION

Figure 1 is the phase diagram about the effect of particles sizes ($\sigma_{\rm AB}$ and $\sigma_{\rm AA}$) on the self-assembly structures in the system of B particles with the same charges (all B particles are negatively charged and have only

DOI:10.1063/1674-0068/27/04/419-427

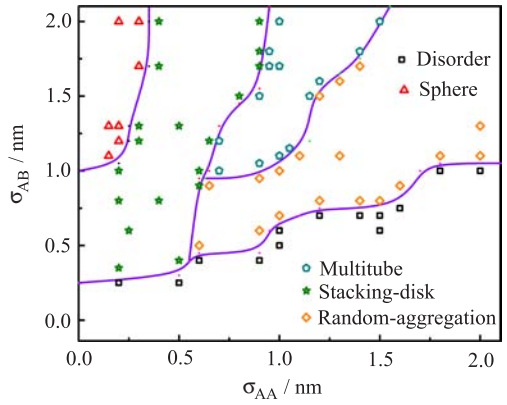

FIG. 1 The phase diagram of the binary particles system controlled by the particles size parameters σ_{AA} and σ_{AB}. The system contains A and B type particles and all B particles have the same negative charges.

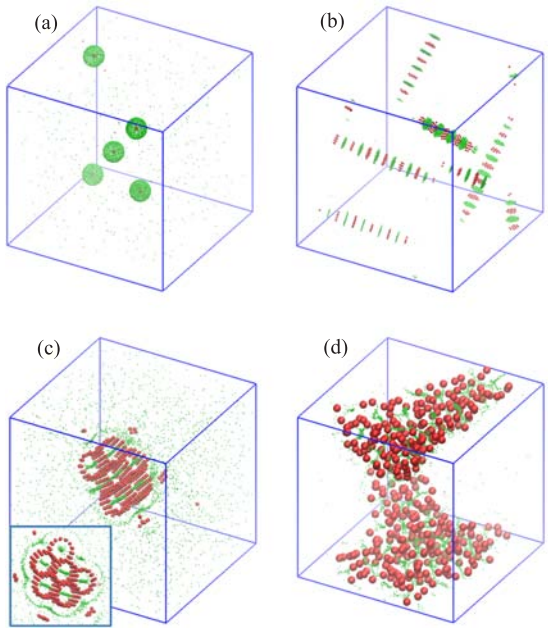

FIG. 2 Typical aggregation structures in the phase diagram (Fig.1) of the binary particles system: (a) sphere, σ_{AA}=0.15 nm, σ_{AB}=1.3 nm, (b) stacking-disk, σ_{AA}=0.5 nm, σ_{AB}=1.3 nm, (c) multitube, σ_{AA}=1 nm, σ_{AB}=1.7 nm, and (d) random aggregations, σ_{AA}=2 nm, σ_{AB}=2 nm. The insert picture represents the front view of the multitube structure in (c). The colours of A and B particles are red and green, respectively.

repulsive interactions from each other). In this phase diagram, the interaction strengths ε_{AA} and ε_{AB} are fixed and ε_{AB} is larger than ε_{AA}. Various structures such as sphere, stacking-disk, multitube, and random-aggregation are observed (the typical structures are shown in Fig.2). The phase diagram shows that the particles sizes (σ_{AB} and σ_{AA}) strongly affect the final aggregation strcutures. When σ_{AB} is small (corresponding to the bottom of the phase diagram), the particles are dispersed because of the repulsive interaction from charged B particles. With σ_{AB} increasing (about σ_{AB}>0.25 nm), differently ordered structures appear depending on σ_{AA}, *i.e.*, the size of A particle. The spherical micellar-like aggegation (Fig.2(a)) is observed at 1 nm<σ_{AB}≤2 nm and σ_{AA}≤0.35 nm (the upper left corner of the phase diagram). In such spherical structure, A particles with the average number C_A≈76 aggregate to form a small cluster and B particles surround the outside of the cluster. In the range of 0.25 nm≤σ_{AB}≤2 nm, a hierarchical structure, *i.e.*, stacking-disk (the monolayers of A and B particles packing alternatively into a rodlike structure) is found at 0.35 nm<σ_{AA}≤0.9 nm (Fig.2(b)), and the average number of A particles for each monolayer disk is C_A≈11. When σ_{AA} increases to 0.9 nm<σ_{AA}<1.5 nm and 0.9 nm<σ_{AB}<2 nm, a novel aggregation structure with multitube is created (Fig.2(c)). In this structure, partial B particles distribute at the inner of each tube to form a line. Other B particles surround the multitube structure. Further increasing σ_{AA} to 1 nm≤σ_{AA}≤2 nm at the upper right corner of the phase diagram, a random aggregation body with A and B particles is formed (Fig.2(d)).

In the system of B particles with the same negative charges and ε_{AB}>ε_{AA}, A particles have a priority to contact with B particles. The repulsion force between B particles prevents the aggregation of A particles depending on σ_{AB} and σ_{AA} (increasing σ_{AB} or decreasing σ_{AA} favors the aggregation of A particles and the aggregation number C_A of A particles increases). Becasue B particles have the pure repulsion from each other, the repulsive effect becomes stronger with σ_{AB} decreasing and the particles are dispersed at small σ_{AB}. Two parameters (σ_{AB} and σ_{AA}) determine the aggregation structures. The equilibrium distance between A and B particles $r_{min-AB}=2^{1/6}\sigma_{AB}$ determines the number of B particles around A particles. Usually, binary particles tend to form an alternating multilayer (stacking-disk) structure in the case of the strong cross-interacton ε_{AB}. But the layer size is limited because of the stronger attraction along the perpendicular direction of layers than that of the layer boundary during aggregation. The simulation shows that the formation of the stacking-disk structure is a gowth process according to the trajectory of structure evolution (Fig.3(a)). The similar strcutures have been observed in the system of block copolymers [61−64]. Two components in block copolymers have similar properties with the binary particles used in our system though they in block copolymers are connected by covalent bonds. When decreasing σ_{AA} from the stacking-disk structure, it is easy to form spherical micelle and the final aggregation body is a mono-shell structure with B particles surrounding the spherical cluster of A particles. The self-assembly trajectory is shown in Fig.3(b). When increasing σ_{AA}

DOI:10.1063/1674-0068/27/04/419-427

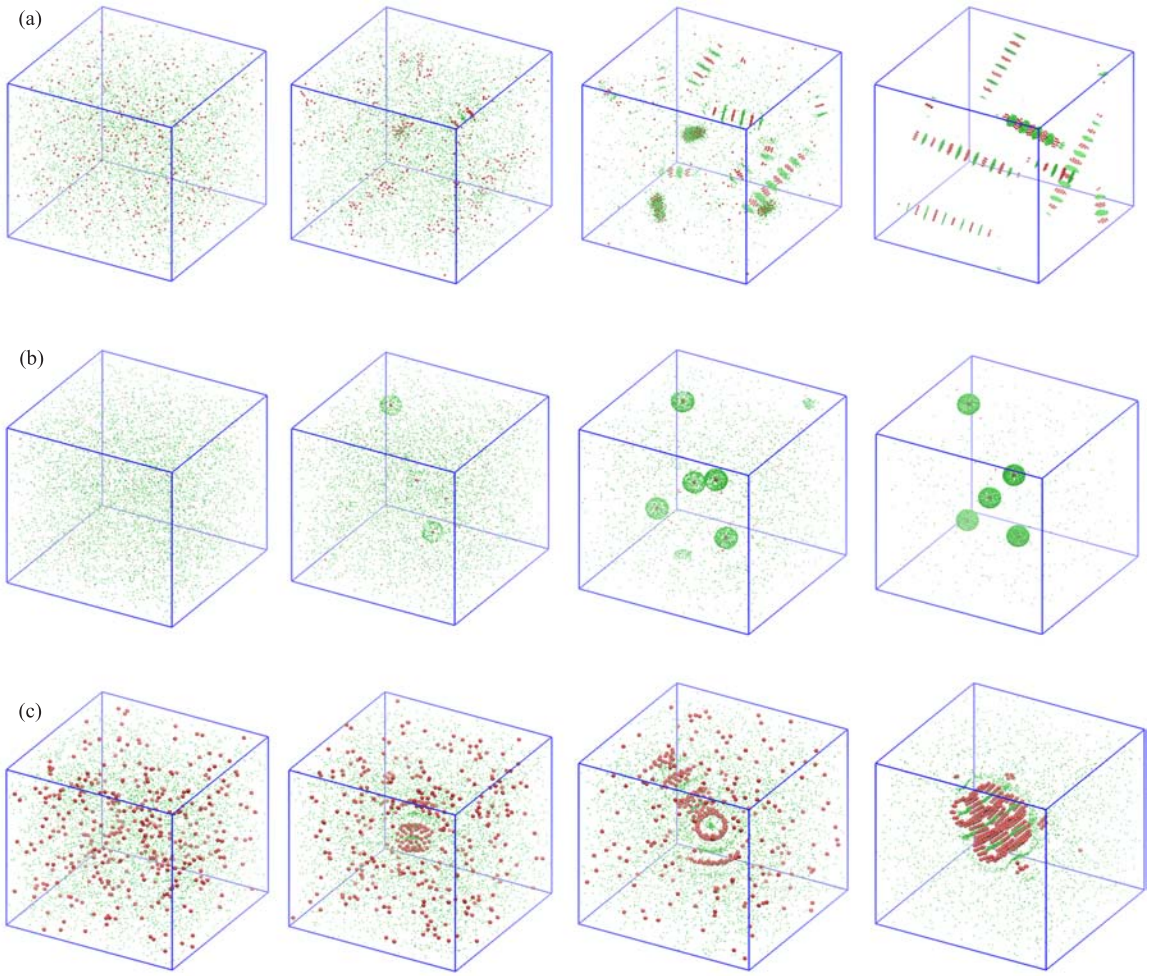

FIG. 3 The formation trajectories of three typical nanostructures: stacking-disk (a), sphere (b), and multitube (c) in annealing processes. The system contains A (red) and B (green) type particles and all B particles have the same negative charges. The simulation parameters are (a) σ_{AA}=0.5 nm and σ_{AB}=1.3 nm, (b) σ_{AA}=0.15 nm and σ_{AB}=1.3 nm, (c) σ_{AA}=1 nm and σ_{AB}=1.7 nm.

from the stacking-disk structure, the structure of A particle layers is not stable and A layer bends into a tube structure. The tubes contact through B particles to form a multitube structure. The inner B particles are forced to form a line and others locate at the outside. The formation process of the multitube structure is also shown in Fig.3(c). While increasing σ_{AA} from the multitube structure, the random-aggregation structure appears and the charged B particles locate at the gaps of the network structures from A particles (Fig.2(d)).

The self-assembly of binary particles in $\varepsilon_{AB}>\varepsilon_{AA}$ is similar to that of the amphiphilic molecules or diblock copolymers (A particles with the attractive interactions can be regarded as the hydrophobic parts and charged B particles with the repulsive force are similar to the hydrophilic parts). The self-assemblies of amphiphilic molecules and diblock copolymers can be understood using the volume packing fraction of compositions [65, 66]. Using the similar way, the packing theory can be used to explain the aggregation structures of binary particles systems with electrostatic and van der Waals interactions. The spherical structure in the present system is similar to the spherical micelle in an amphiphilic molecule system. The packing parameter p in the amphiphilic molecules system is

$$p = \frac{v}{a_0 l_c} \tag{6}$$

where v is the volume of the hydrocarbon chain or chains, a_0 is called as the optimal area of each headgroup in the molecules and l_c is the critical chain length of an amphiphilic molecule. The packing theory predicts that the spherical micelle forms at $p<1/3$ [65]. In present binary particle system, the conventional p can be expressed as:

$$p = \frac{Mv}{Ma_0 l_c} = \frac{V}{Sl_c} \tag{7}$$

where M and V are the total number and total volume of the amphiphilic molecules in the system, respectively.

DOI:10.1063/1674-0068/27/04/419-427

S is the total optimal area of head-groups (B particles in this system) in all amphiphilic molecules

$$S = \pi \left(\frac{\sigma'_{\mathrm{BB}}}{2}\right)^2 N_{\mathrm{B}} \tag{8}$$

where σ'_{BB} is the real distance between B particles. l_{c} is approximately equal to σ'_{AB} (the real distance between A particles and B particles). Here, V includes three parts: the total volume of A particles V_{A}, the total volume of B particles V_{B} and the total volume of the space between A and B particles V_{AB} caused by $r_{\text{min-AB}}$. As a result,

$$V = V_{\mathrm{A}} + V_{\mathrm{B}} + V_{\mathrm{AB}} \tag{9}$$

$$V_{\mathrm{A}} = \frac{4}{3}\pi \left(\frac{\sigma'_{\mathrm{AA}}}{2}\right)^3 N_{\mathrm{A}} \tag{10}$$

$$V_{\mathrm{B}} = \frac{4}{3}\pi \left(\frac{\sigma'_{\mathrm{BB}}}{2}\right)^3 N_{\mathrm{B}} \tag{11}$$

$$V_{\mathrm{AB}} = \pi \left(\frac{\sigma'_{\mathrm{AA}}}{2}\right)^2 \left(\sigma'_{\mathrm{AB}} - \frac{\sigma'_{\mathrm{AA}}}{2} - \frac{\sigma'_{\mathrm{BB}}}{2}\right) N_{\mathrm{A}} \tag{12}$$

where V_{AB} is total volume with the cross-sectional area of A particles. σ'_{AA} is the real distance between A particles. σ'_{AA}, σ'_{BB}, and σ'_{AB} are measured by the radial distribution functions (see Fig.4(c)). N_{A} and N_{B} are the numbers of A and B particles, N_{A}=400 and N_{B}=5800, respectively. The binary particles can be regarded as pseudo amphiphilic molecules and each of them consists of one A particle and 14.5 B particles. p can be calculated with the particles concentrations and radial distribution functions. The result shows that $p \approx 0.21 < 1/3$ (σ'_{AA}=0.130 nm, σ'_{BB}=0.082 nm and σ'_{AB}=1.248 nm in Fig.4(a)) for the spherical aggregation structure. It indicates that the classical packing theory is still suitable for explaining the simple nanostructures formation in present binary particles system. However, the packing theory (Eq.(7)) is no longer feasible for the complex hierarchical structures such as the stacking-disk or multitube structure. Instead of that, the self-assembly rules of diblock copolymers can be employed to explain the structures formation. The structures of stacking-disk and multitube in present system are similar to the lamellar and cylindrical phase structures of diblock copolymer in bulk. In the melting system of diblock copolymer, the equilibrium phase structure mainly depends on the volume fraction f_{A} of one block in a diblock copolymer [66]. Under the condition of the strong phase segregation, the lamellar and cylindrical phase structures locate at $0.30 < f_{\mathrm{A}} < 0.65$ and $0.65 \leq f_{\mathrm{A}} < 0.85$ for diblock copolymers. In the present system of binary particles, f_{A} of A particles in an aggregation body can be used as a reference variable to understand the phase structure formation. The binary particles are regarded as the diblock copolymers (one A particle and 14.5 B particles for each diblock copolymer). f_{A} is calculated

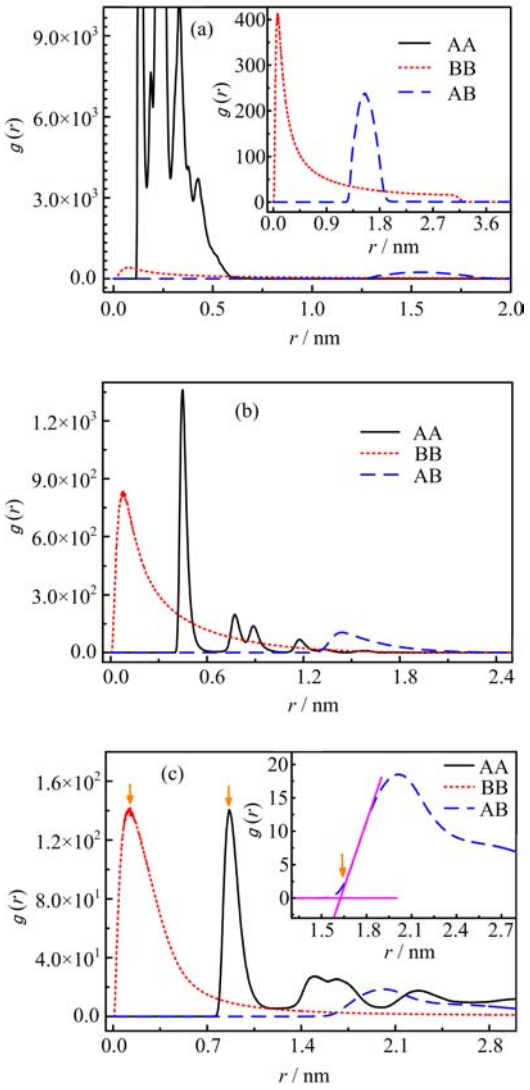

FIG. 4 The radial distribution functions of three typical structures: (a) sphere, (b) stacking-disk, and (c) multitube. This binary particles system contains A and B particles and all B particle have the same negative charges. The corresponding parameters are (a) σ_{AA}=0.15 nm and σ_{AB}=1.3 nm, (b) σ_{AA}=0.5 nm and σ_{AB}=1.3 nm, (c) σ_{AA}=1.0 nm and σ_{AB}=1.7 nm. The selection method of σ'_{AA}, σ'_{BB} and σ'_{AB} is indicated by the arrows in (c).

from three parameters V_{A}, V_{B}, and V_{AB}:

$$f_{\mathrm{A}} = \frac{V_{\mathrm{A}} + \frac{1}{2}V_{\mathrm{AB}}}{V_{\mathrm{A}} + V_{\mathrm{B}} + V_{\mathrm{AB}}} \tag{13}$$

The result shows $f_{\mathrm{A}} \approx 0.61$ for the stacking-disk structure (σ'_{AA}=0.471 nm, σ'_{BB}=0.082 nm, σ'_{AB}=1.300 nm in Fig.4(b)) and $f_{\mathrm{A}} \approx 0.66$ for the multitube structure (σ'_{AA}=0.864 nm, σ'_{BB}=0.131 nm and σ'_{AB}=1.630 nm in Fig.4(c)). It is consistent with the phase structure distribution of diblock copolymer in its phase diagram. The estimation of p and f_{A} in the binary particles system is helpful to determine the particle aggregation

DOI:10.1063/1674-0068/27/04/419-427

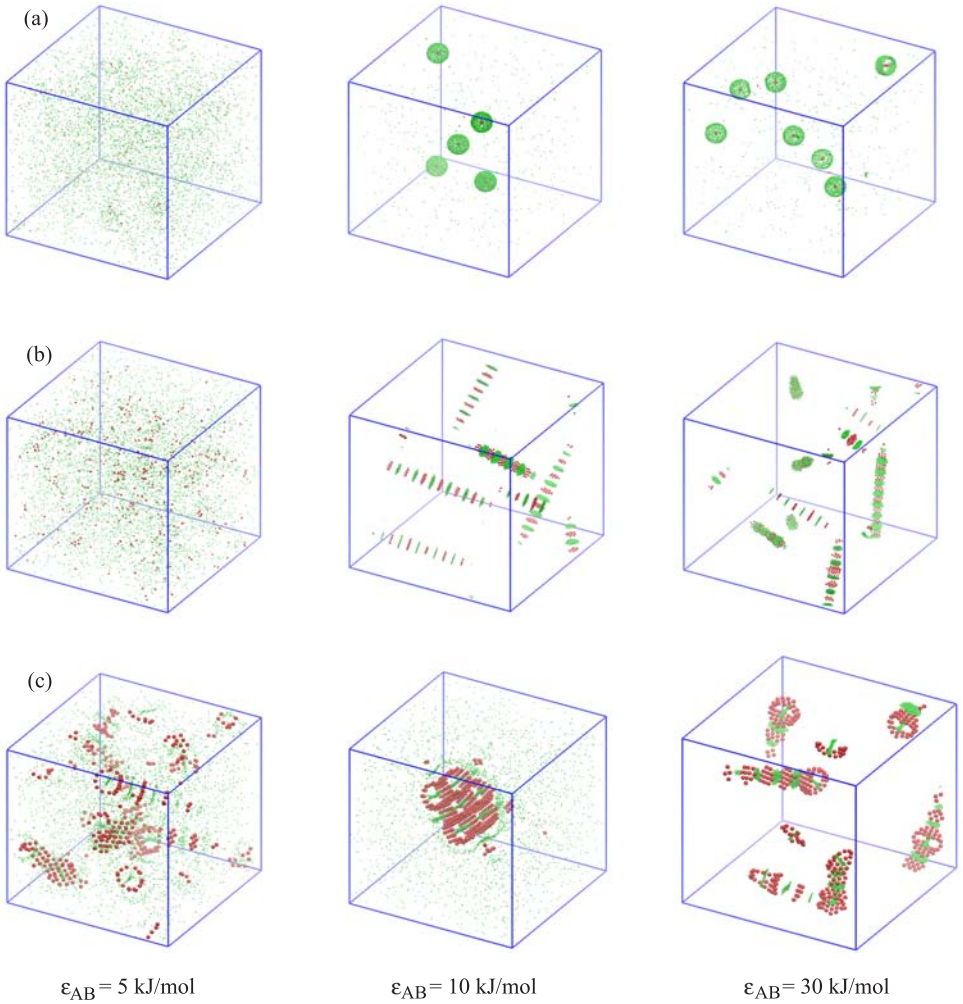

FIG. 5 The structures transformations of the sphere (a), stacking-disk (b) and multitube (c) with changing ε_{AB} from 5 kJ/mol to 30 kJ/mol. Here, ε_{AA} is fixed and equals to 4 kJ/mol. The A and B particles are represented with red and green colours, respectively.

structure.

In order to explore the influence of the interaction strength, the interaction strength ε_{AA} between A particles is changed from 2 kJ/mol to 10 kJ/mol and the cross-interaction strength ε_{AB} between A particles and B particles is changed from 5 kJ/mol to 30 kJ/mol to illustrate the structure transformations of three typical structures (sphere, stacking-disk, and multitube). The results show that the change of ε_{AA} does not cause the phase transformation when ε_{AB}=10 kJ/mol. However, the change of ε_{AB} strongly affects the structure formation when ε_{AA}=4 kJ/mol. Figure 5 shows the structure transformation of typical aggregation bodys (sphere, staking-disk, and multitube) with the change of ε_{AB}. For the spherical structure, the aggregation disappears as ε_{AB} decreases from 10 kJ/mol to 5 kJ/mol. When ε_{AB} increases to 30 kJ/mol, the spherical structure of A particles does not change. The multitube structure disappears when ε_{AB}=5 kJ/mol but it transforms into the stacking-disk structure when ε_{AB} is changed as 30 kJ/mol. The stacking-disk structure does not change with ε_{AB} increasing and becomes unstable as ε_{AB} decreases. It indicates that the cross-interaction ε_{AB} is important to the formation of rich structure. With ε_{AB} increasing, the binary particles are more favable to aggregate because A particles favor interacting with B particles.

Figure 6 shows the phase diagram of the system with the same amount of positive and negative charged B particles (q_B=±0.6e). The whole system is electrically neutral. Four kinds of structures, disorder, stacking-disk, tube and random-aggregation, are observed (Fig.7). Different from the phase diagram in Fig.1, the spherical structure disappears. The tube structure in the new phase diagram has a slight difference from the multitube structure in Fig.1. In Fig.6, A particles only assemble into the single tube structure which is shorter than those in Fig.1. The reason is that the particles aggregation is affected by the annealing rates. The multitube aggregation would appear again

DOI:10.1063/1674-0068/27/04/419-427

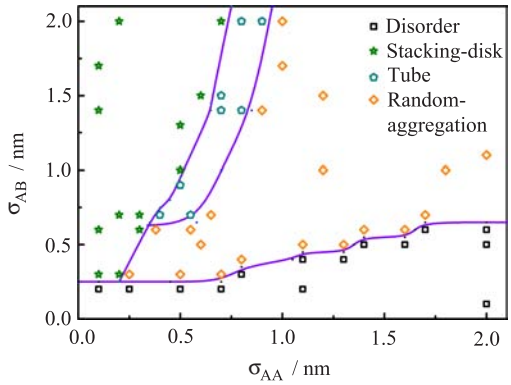

FIG. 6 The phase diagram of binary particles system controlled by the particles size parameters σ_{AA} and σ_{AB}. In this system, B particles have opposite charges and the system is electrically neutral.

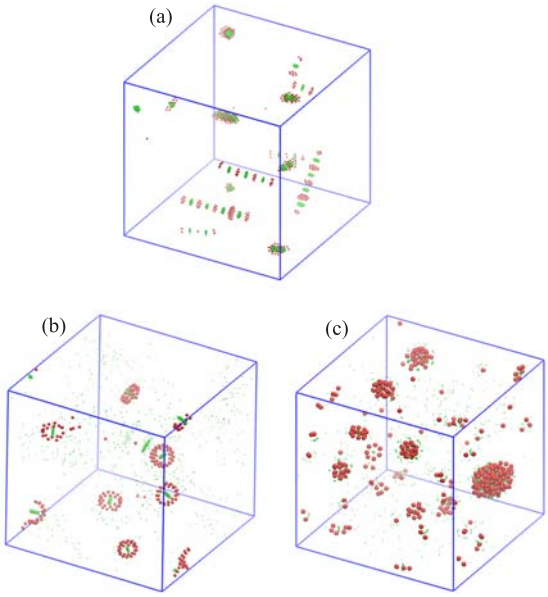

FIG. 7 Typical aggregation structures in Fig.6. (a) Stacking-disk, σ_{AA}=0.5 nm, σ_{AB}=1.3 nm, (b) tube, σ_{AA}=0.8 nm, σ_{AB}=1.4 nm, and (c) random-aggregation σ_{AA}=1.2 nm, σ_{AB}=1 nm. In such system, B particles have opposite charges and the system is electrically neutral. The colours of A and B particles are red and green, respectively.

if the annealing rate is slow enough. However, it needs much longer time beyond our tolerance. Figure 6 shows that all the phase structures start to appear at lower σ_{AB} compared with those in Fig.1. It is believed that introducing opposite ions reduces the effect of repulsive interaction between B particles and decreases the balance distance between B particles. As a result, the attractive effect between A and B particles is relatively strengthened. So, the similar structures should appear at lower σ_{AB}, *i.e.*, the phase regions move to lower σ_{AB}. It is found that B particles tend to form a core in the most structures. It is reasonable that when B particles with positive and negative charges are added, B particles aggregate into salt under the electrostatic attraction. Comparing the phase diagrams of the two systems (Fig.1 and Fig.6), the distributions of typical structures appear an offset in the electrically neutral system because introducing the opposite ions changes the competitive relationship between binary particles.

The past experiments have shown that adding electrolytes can induce the aggregations of some particles in solution. *n*-C_{60} particles [55], titanium dioxide particles [67] or polystyrene spheres [68] can aggregate when adding electrolytes in solution. In these systems, the interaction between the positive ions and particles is stronger and the positive ions favor contacting with the particles when the electrolyte is introduced. Afterwards, particles aggregate to decrease the free-energy of the system. The classical Derjauin-Landau-Verwey-Overbeek (DLVO) theory explains that introducing electrolyte changes the repulsive effect of particles in the system and results in the particle aggregation. Our simulation results are consistent with the theoretical results. Meanwhile, the simulation shows that the relatively strong cross-interaction is important for the formation of complex and ordered aggregation structures. In experiments, the strong cross-interaction can be realized by bridging hydrogen bonds and the strength of the cross-interaction may be tuned by changing the number of hydrogen bonds [69]. The novel aggregation structures are possibly observed in future experiments by tuning the cross-interaction and size of particles.

IV. CONCLUSION

In this work, the particle Langevin dynamics simulation is employed to explore the self-assembly of binary particles with the electrostatic and van der Waals interactions in solution. Under the strong cross-interactions of binary particles, the rich aggregation structures such as stacking-disk, sphere and tube structures can be found by changing the particle sizes (σ_{AB} and σ_{AA}). The typical aggregation structures are further explained with the self-assembly rules of amphphilic molecules or diblock copolymers and the computation results are consistent with the prediction of the modified packing theory. Adding opposite ions moves the phase regions in the phase diagram to lower σ_{AB}. These results provide valuble information for understanding the formation and transformation of complex aggregation structures of multicomponent particles in solution.

V. ACKNOWLEDGMENTS

The computer simulation is performed on the High Performance Computing Center of Tianjin University,

DOI:10.1063/1674-0068/27/04/419-427

China. This work was supported by the National Natural Science Foundation of China (No.21274107 and No.91127046). We thank Prof. Bin Zhang, Rui Xu, Bo Du, and Dr. Zi-lu Wang in Tianjin University for helpful discussions.

[1] L. M. Liz-Marzán and P. Mulvaney, J. Phys. Chem. B **107**, 7312 (2003).
[2] A. P. Alivisatos, Science **271**, 933 (1996).
[3] D. V. Talapin, J. S. Lee, M. V. Kovalenko, and E. V. Shevchenko, Chem. Rev. **110**, 389 (2010).
[4] Z. Nie, A. Petukhova, and E. Kumacheva, Nat. Nano **5**, 15 (2010).
[5] W. Cho, Y. H. Lee, H. J. Lee, and M. Oh, Adv. Mater. **23**, 1720 (2011).
[6] S. Srivastava and N. A. Kotov, Soft Matter **5**, 1146 (2009).
[7] J. Wang, H. Xia, Y. Zhang, H. Lu, R. Kamat, A. V. Dobrynin, J. Cheng, and Y. Lin, J. Am. Chem. Soc. **135**, 11417 (2013).
[8] S. J. Liu, Y. J. Li, Y. M. Wang, X. Liu, and E. S. Yeung, J. Colloid Interface Sci. **407**, 243 (2013).
[9] M. R. Jones, K. D. Osberg, R. J. Macfarlane, M. R. Langille, and C. A. Mirkin, Chem. Rev. **111**, 3736 (2011).
[10] S. Liang, X. L. Liu, Y. Z. Yang, Y. L. Wang, J. H. Wang, Z. J. Yang, L. B. Wang, S. F. Jia, X. F. Yu, L. Zhou, J. B. Wang, J. Zeng, Q. Q. Wang, and Z. Zhang, Nano Lett. **12**, 5281 (2012).
[11] H. Zhang and D. Wang, Angew. Chem. Int. Ed. **47**, 3984 (2008).
[12] S. Sacanna, D. J. Pine, and G. R. Yi, Soft Matter **9**, 8096 (2013).
[13] S. J. Hurst, E. K. Payne, L. Qin, and C. A. Mirkin, Angew. Chem. Int. Ed. **45**, 2672 (2006).
[14] D. Seo, C. I. Yoo, J. Jung, and H. Song, J. Am. Chem. Soc. **130**, 2940 (2008).
[15] Y. Sun and Q. Wang, Soft Matter **9**, 2172 (2013).
[16] L. Qin, S. Park, L. Huang, and C. A. Mirkin, Science **309**, 113 (2005).
[17] J. Yao, Z. Liu, Y. Liu, Y. Wang, C. Sun, G. Bartal, A. M. Stacy, and X. Zhang, Science **321**, 980 (2008).
[18] J. Xu, L. Chen, H. Choi, H. Konish, and X. Li, Sci. Rep. **3**, 1730 (2013).
[19] T. Ung, L. M. Liz-Marzán, and P. Mulvaney, Langmuir **14**, 3740 (1998).
[20] D. I. Gittins, A. S. Susha, B. Schoeler, and F. Caruso, Adv. Mater. **14**, 508 (2002).
[21] M. Giersig, T. Ung, L. M. Liz-Marzán, and P. Mulvaney, Adv. Mater. **9**, 570 (1997).
[22] J. Yang, E. H. Sargent, S. O. Kelley, and J. Y. Ying, Nat. Mater. **8**, 683 (2009).
[23] L. M. Liz-Marzán, M. Giersigb, and P. Mulvaney, Chem. Commun. **6**, 731 (1996).
[24] R. Bardhan, S. Mukherjee, N. A. Mirin, S. D. Levit, P. Nordlander, and N. J. Halas, J. Phys. Chem. C **114**, 7378 (2010).
[25] P. Mulvaney, L. M. Liz-Marzán, M. Giersigc, and T. Ung, J. Mater. Chem. **10**, 1259 (2000).
[26] L. M. Liz-Marzán, M. Giersig, and P. Mulvaney, Langmuir **12**, 4329 (1996).
[27] V. Mazumder, M. Chi, K. L. More, and S. Sun, Angew. Chem. Int. Ed. **49**, 9368 (2010).
[28] S. Fullam, D. Cottell, H. Rensmo, and D. Fitzmaurice, Adv. Mater. **12**, 1430 (2000).
[29] J. W. Kim, E. I. Galanzha, E. V. Shashkov, H. M. Moon, and V. P. Zharov, Nat. Nano. **4**, 688 (2009).
[30] J. J. Baumberg, T. A. Kelf, Y. Sugawara, S. Cintra, M. E. Abdelsalam, P. N. Bartlett, and A. E. Russell, Nano Lett. **5**, 2262 (2005).
[31] M. R. Jones, R. J. Macfarlane, B. Lee, J. Zhang, K. L. Young, A. J. Senesi, and C. A. Mirkin, Nat. Mater. **9**, 913 (2010).
[32] P. C. Millett and Y. U. Wang, Acta Mater. **57**, 3101 (2009).
[33] D. A. Walker, K. P. Browne, B. Kowalczyk, and B. A. Grzybowski, Angew. Chem. Int. Ed. **49**, 6760 (2010).
[34] R. Zangi and B. J. Berne, J. Phys. Chem. B **110**, 22736 (2006).
[35] Y. L. Zhu and Z. Y. Lu, J. Chem. Phys. **134**, 44903 (2011).
[36] W. Tian and Y. Ma, J. Phys. Chem. B **113**, 1361 (2009).
[37] Y. Li, X. Zhang, and D. Cao, J. Phys. Chem. B **117**, 6733 (2013).
[38] D. Suzuki and K. Horigome, Langmuir **27**, 12368 (2011).
[39] S. Williams, C. Royall, and G. Bryant, Phys. Rev. Lett. **100**, 225502 (2008).
[40] K. P. Velikov, C. G. Christova, R. P. Dullens, and A. van Blaaderen, Science **296**, 106 (2002).
[41] K. N. Pham, A. M. Puertas, J. Bergenholtz, S. U. Egelhaaf, A. Moussaid, P. N. Pusey, A. B. Schofield, M. E. Cates, M. Fuchs, and W. C. Poon, Science **296**, 104 (2002).
[42] M. Dijkstra, R. van Roij, and R. Evans, Phys. Rev. Lett. **81**, 2268 (1998).
[43] S. Ilett, A. Orrock, W. Poon, and P. Pusey, Phys. Rev. E **51**, 1344 (1995).
[44] M. Dijkstra, R. van Roij, and R. Evans, Phys. Rev. E **59**, 5744 (1999).
[45] D. Zhang, Y. Jiang, X. Wen, and L. Zhang, Soft Matter **9**, 1789 (2013).
[46] L. Filion and M. Dijkstra, Phys. Rev. E **79**, 46714 (2009).
[47] F. X. Redl, K. S. Cho, C. B. Murray, and S. O'Brien, Nature **423**, 968 (2003).
[48] E. Trizac, M. D. Eldridge, and P. A. Madden, Mol. Phys. **90**, 675 (1997).
[49] M. D. Eldridge, P. A. Madden, P. N. Pusey, and P. Bartlett, Mol. Phys. **84**, 395 (1995).
[50] M. D. Eldridge, P. A. Madden, and D. Frenkel, Mol. Phys. **79**, 105 (1993).
[51] M. D. Eldridge, P. A. Madden, and D. Frenkel, Mol. Phys. **80**, 987 (1993).
[52] Z. Chen, J. Li, X. Zhang, Z. Wu, H. Zhang, H. Sun, and B. Yang, Phys. Chem. Chem. Phys. **14**, 6119 (2012).
[53] Z. Tang, Z. Zhang, Y. Wang, S. C. Glotzer, and N. A. Kotov, Science **314**, 274 (2006).
[54] Q. Tang and Y. Ma, J. Phys. Chem. B **113**, 10117 (2009).
[55] J. Brant, H. Lecoanet, and M. R. Wiesner, J. Nanopart.

DOI:10.1063/1674-0068/27/04/419-427

Res. **7**, 545 (2005).
[56] S. Bhattacharjee, M. Elimelech, and M. Borkovec, Croat. Chem. Acta **71**, 883 (1998).
[57] Z. D. Zhang, X. H. He, and S. C. Jiang, Chin. J. Polym. Sci. **30**, 744 (2012).
[58] R. Xu, Z. L. Wang, H. P. Li, and X. H. He, Chin. J. Chem. Phys. **26**, 203 (2013).
[59] M. Camargo, A. J. Moreno, and C. N. Likos, J. Stat. Mech. **10**, 10015 (2010).
[60] B. Hess, C. Kutzner, D. van der Spoel, and E. Lindahl, J. Chem. Theory Comput. **4**, 435 (2008).
[61] S. J. Jeon, G. R. Yi, and S. M. Yang, Adv. Mater. **20**, 4103 (2008).
[62] R. Deng, F. Liang, W. Li, Z. Yang, and J. Zhu, Macromolecules **46**, 7012 (2013).
[63] H. Cui, Z. Chen, S. Zhong, K. L. Wooley, and D. J. Pochan, Science **317**, 647 (2007).
[64] P. Chi, Z. Wang, B. Li, and A. C. Shi, Langmuir **27**, 11683 (2011).
[65] J. N. Israelachvili, D. J. Mitchell, and B. W. Ninham, J. Chem. Soc. Faraday Trans. **72**, 1525 (1976).
[66] F. S. Bates and G. H. Fredrickson, Phys. Today **52**, 32 (1999).
[67] R. A. French, A. R. Jacobson, B. Kim, S. L. Isley, R. L. Penn, and P. C. Baveye, Environ. Sci. Technol. **43**, 1354 (2009).
[68] D. Majolino, F. Mallamace, P. Migliardo, N. Micali, and C. Vasi, Phys. Rev. A **40**, 4665 (1989).
[69] T. Coradin, S. Bah, and J. Livage, Colloids Surf. B **35**, 53 (2004).

DOI:10.1063/1674-0068/27/04/419-427